

SIMULATION OF POLYMERIC FLOW IN A TWIN-SCREW EXTRUDER: AN ANALYSIS OF ELONGATIONAL VISCOSITY EFFECTS

*A. Shah and M. Gupta
Mechanical Engineering-Engineering Mechanics Department
Michigan Technological University
Houghton, MI 49931*

Abstract

Flow of a polymer in an intermeshing co-rotating twin-screw extruder is simulated. Effect of elongational viscosity on the flow is analyzed using independent power-law models for the shear and elongational viscosities. Axial component of the velocity is found to be maximum in the intermeshing region of the extruder. Axial component of velocity, which determines the throughput of the extruder, decreased as the elongational viscosity of the polymer used for the flow simulation was increased. The pressure in the extruder decreased from a very high positive value on the leading edge to a very large negative value on the trailing edge of the screw. For the same rotational speed the pressure build-up in the twin-screw extruder increased as the elongational viscosity of the polymer was increased.

Introduction

In plastic industry, single- and twin-screw extruders [1, 2] are commonly used to melt and pump a polymer through a die. Besides melting and pumping, extruders also perform other functions such as mixing, compounding, chemical reaction, devolatilization. The flow in a single-screw extruder is induced by the friction between the barrel and the polymer, whereas in an intermeshing twin-screw extruder along with this drag-induced flow in the translational region, a positive displacement flow is also obtained in the intermeshing region between the two screws. Because of this positive displacement flow, intermeshing twin-screw extruders are preferred for polymers such as polyvinylchloride (PVC), which have poor flow characteristics and are susceptible to thermal degradation. Even though, counter-rotating twin-screw extruders provide more positive displacement than the extruders with co-rotating twin screws, co-rotating screws are commonly used because of their modular nature, which allows interchangeable screw elements, and because of the possibility of a self-wiping screw profile.

In comparison to the flow in a twin-screw extruder, the flow in a single-screw extruder is simple, and is also easier to simulate numerically because a stationary flow domain can be obtained by fixing the coordinate frame on the rotating screw of the single-screw extruder. Since such a simplification cannot be performed for twin-screw

extruders, relatively fewer attempts have been made in the literature for a full three-dimensional simulation of the flow in twin-screw extruders. Instead, many attempts for flow simulation in twin-screw extruders employ Flow Analysis Network (FAN) technique, which simplifies the simulation by using the lubrication approximation [3, 4]. Recently some attempts have been made for full three-dimensional simulation of the polymeric flow in the kneading blocks [5 – 8] and also in full-flighted screws [9, 10]. Most of these finite element simulations used a fixed mesh for a particular configuration of the two screws or kneading blocks. Some of the recent publications [6, 9, 10] have used mesh superposition method, which uses a fixed mesh inside the barrel and determines the flow domain by superimposing the mesh in the barrel with the meshes in the screws. With the mesh superposition method, flow in different screw configurations can be simulated with the same set of finite element meshes.

In single-screw extruders, the drag-induced flow is primarily shear dominated, whereas the flow in the intermeshing region of a twin-screw extruder is significantly elongational in nature. The elongational flow in the intermeshing region is the main reason for better mixing and compounding capability of twin-screw extruders. In general, an elongational flow has a better mixing efficiency than a shear flow [2]. Because of the elongational nature of the flow in the intermeshing region, for an accurate simulation of the flow in a twin-screw extruder, it is important to account for the effect of elongational viscosity on the flow.

Geometry of the Twin-Screw Extruder

The dimensions of the two screws and the barrel used in the present work, which are shown in Fig. 1, were adopted from the dimensions of the two-lobe kneading discs used by Ishikawa et al. [7]. The cross-sectional dimensions of the kneading discs used by Ishikawa et al., were rotated with a screw lead of 30 mm (that is, screw pitch = 15 mm) to obtain a self-wiping co-rotating twin-screw extruder. As shown in Fig. 1, the two-lobe cross-section was rotated through 540° to obtain 45 mm axial length of the two screws. For the flow simulation reported later in this paper, the two screws were rotated at 60 RPM.

Shear and Elongational Viscosity Models

In the present work, the PELDOM software [11] is used to analyze the effect of elongational viscosity on the flow in the twin-screw extruder geometry discussed above. Besides the shear viscosity, to simulate a three-dimensional flow, the software requires a knowledge of the strain-rate dependence of the axisymmetric and planar elongational viscosities of the polymer. Even though the software has provision for using more realistic shear and elongational viscosity models, for simplicity, the truncated power-law model is used in the present work for the shear as well as the elongational viscosities.

$$\eta_s = Ae_{II}^{n-1} \quad \text{for } e_{II} \geq e_0, \quad \eta_s = \eta_0 \quad \text{for } e_{II} \leq e_0$$

$$\eta_a = Be_{II}^{m_a-1} \quad \text{for } e_{II} \geq e_0, \quad \eta_a = 3\eta_0 \quad \text{for } e_{II} \leq e_0$$

and

$$\eta_p = Ce_{II}^{m_p-1} \quad \text{for } e_{II} \geq e_0, \quad \eta_p = 4\eta_0 \quad \text{for } e_{II} \leq e_0$$

where η_s is the shear viscosity, η_a and η_p are respectively the axisymmetric and planar elongational viscosities, η_0 is the zero-shear viscosity, n , m_a and m_p are the power-law indices, and A , B and C are the consistency coefficients. For the polymer used in this work, the shear viscosity parameters are $A = 53,681 \text{ Pa}\cdot\text{s}^{0.27}$, $n = 0.27$ and $e_0 = 1.85 \times 10^{-4} \text{ s}^{-1}$.

Results and Discussion

The finite element mesh used to simulate the flow in the twin-screw extruder is shown in Fig. 2. The finite element mesh has 15,309 nodes and 54,615 tetrahedral finite elements. Even though, the flow domain in the twin-screw extruder is quite complex, since tetrahedral elements are used in the present work, in comparison to a mesh with brick elements, the finite element mesh generation is relatively easy. The $P_1^+P_1$ finite element, which uses linear interpolation for pressure and a linear interpolation enriched with a bubble node at the centroid for velocity [12], was used for the flow simulation. For improved efficiency, the velocity equations for the bubble nodes were eliminated at the element level by using the static condensation technique [13]. It was mentioned earlier that for the flow simulation screws were rotated at 60 RPM. The circumferential velocity based upon the rotational speed of 60 RPM was specified on the nodes on the screw surfaces, whereas the no-slip condition was enforced on the barrel surface. No-traction condition was employed at the two ends of the extruder mesh.

Fig. 3 shows the effect of elongational power-law index on the velocity distribution in two of the planes perpendicular to the extruder axis. In Fig. 3 and in all subsequent figures, the polymer enters the extruder at $z = 0$ and the extruder exit is at $z = 45 \text{ mm}$. Arrows in Fig. 3

show the direction of velocity, whereas the magnitude is depicted by the color of the arrow. As expected, in Fig. 3, in the translational regions in the two lobes, the velocity decreases from the screw surface to the barrel surface, whereas in the intermeshing region the fluid is transferred from one lobe to the other lobe. Qualitatively, in Fig. 3, the velocity distributions for the three different values of the elongational power-law index are similar.

Variation of the axial component of velocity for the three different values of the elongational power-law index is shown in Fig. 4. Irrespective of the value of the elongational power-law index, the maximum axial velocity is in the intermeshing region. However, as the elongational power-law index is increased the axial velocity in the intermeshing region decreases. Therefore, for the same rotational speed, the flow rate in an extruder is expected to decrease for a higher elongational power-law index. In the translational region in Fig 4 (a), where the flow is shear dominated, elongational viscosity has only a limited effect on the axial velocity distribution.

In Figs. 4 (a – c), the minimum value of the axial velocity component is zero, indicating that everywhere in the two cross-sections shown, the flow is in the forward direction. However, the predicted axial velocity component at some locations in the intermeshing region at the exit was in the reverse direction. This reverse flow might have resulted from the no-traction boundary condition enforced at the exit, which may not be valid in the intermeshing region. Because of this reverse flow at the exit, even though the software can predict the temperature distribution in a polymeric flow, only an isothermal version of the software was used to simulate the flow in the twin-screw extruder. To solve the energy equation for a non-isothermal flow simulation, temperature at the exit in the regions with reverse flow is required as an input, which is not known. A non-isothermal simulation of the flow in the twin-screw extruder was attempted in the present work, but erroneous temperature was predicted in the regions with reverse flow at the exit.

Fig. 5 shows the pressure distribution in two of the planes perpendicular to the axis of the extruder. The predicted pressure distribution on the barrel surface is shown in Fig. 6. It should be noted that a logarithmic scale has been used for the coloring scheme in Figs. 5 and 6. It is evident from Figs. 5 and 6 that the pressure changes from a very high positive value on the leading edges of the two screws to a very large negative value on the trailing edges. In Fig. 6, in the channel between the two adjacent screw flights, in comparison to the pressure near the two flights, the magnitude of the pressure is small. However, it is evident from Fig. 6 that the pressure in the translational region in this channel between the two adjacent screw flights increases towards the exit. It is also noted that there is a sharp change in the pressure in this channel as the

polymer goes from one lobe to the other lobe of the twin-screw extruder. In general, in Figs. 5 and 6, the predicted pressure in the extruder increases significantly as the elongational power-law index is increased.

It should be noted that for $n = m_a = m_p$, the viscosity model used in the present work, reduces to the truncated power-law model with the generalized Newtonian formulation. Therefore, the velocity and pressure distributions in Figs. 3 (a) – 6 (a) are the same as those predicted by the generalized Newtonian formulation. However, since the elongational viscosity of a polymer is typically higher than the elongational viscosity predicted by the generalized Newtonian formulation, the predictions in Figs. 3 (b, c) – 6 (b, c) may be closer to the actual velocity and pressure distributions in polymeric flows.

Conclusions

Polymeric flow in a twin-screw extruder was simulated. Effect of elongational viscosity on the flow was analyzed. For a fixed shear viscosity, as the elongational viscosity of the fluid was increased, the axial component of velocity, and hence, the throughput of the extruder was found to decrease, whereas the pressure build-up in the extruder increased for the higher elongational viscosity.

References

1. J. L. White, *Twin Screw Extrusion*, Hanser Publishers, New York (1992).
2. D. G. Baird and D. I. Collias, *Polymer Processing*, John Wiley and Sons, Inc. (1998).
3. W. Szydlowski and J. L. White. *Adv. Polym. Tech.*, **7**, 177 (1987).
4. Y. Wang and J. L. White. *J. Non-Newtonian Fluid Mech.*, **32**, 19 (1989).
5. A. Kiani, J. E. Curry and P. G. Anderson, *SPE ANTEC Tech. Papers*, **44**, 48 (1998).
6. B. Alsteens, V. Legat, T. Avalosse and T. Marchal, *SPE ANTEC Tech. Papers*, **44**, 194 (1998).
7. T. Ishikawa, S. Kihara and K. Funatsu, *Polym. Eng. Sci.*, **40**, 357 (2000).
8. V. L. Bravo, A. N. Hrymak, J. D. Wright, *Polym. Eng. Sci.*, **40**, 525 (2000).
9. A. Lawal, S. Railkar and D. M. Kalyon, *SPE ANTEC Tech. Papers*, **45**, 317 (1999).
10. T. Avalosse, Y. Rubin, *SPE ANTEC Tech. Papers*, **45**, 322 (1999).
11. PELDOM software, Plastic Flow, LLC, 1206 Birch Street, Houghton, MI 49931 (www.plasticflow.com).
12. E. Pichelin and T. Coupez, *Comput. Methods Appl. Mech. Eng.*, **163**, 359 (1998).
13. K. J. Bathe, *Finite Element Procedures*, Prentice Hall, New Jersey (1998).

Table 1: Dimensions of the twin-screw extruder.

	(mm)
Barrel Diameter	30.0
Screw tip diameter	29.2
Screw root diameter	21.0
Centerline distance	26.0
Screw lead	30.0

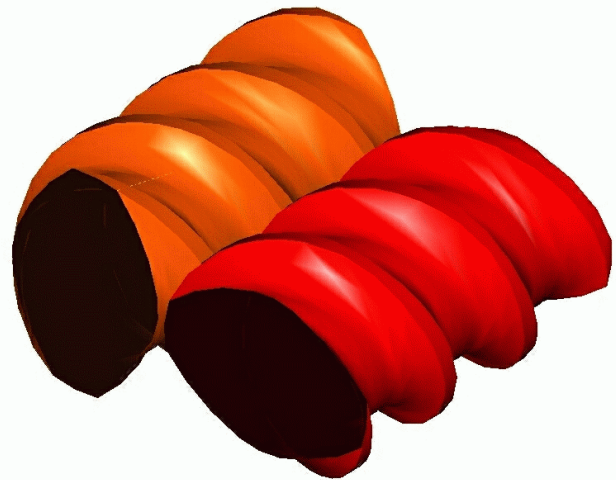


Fig. 1 Geometry of the two intermeshing screws.

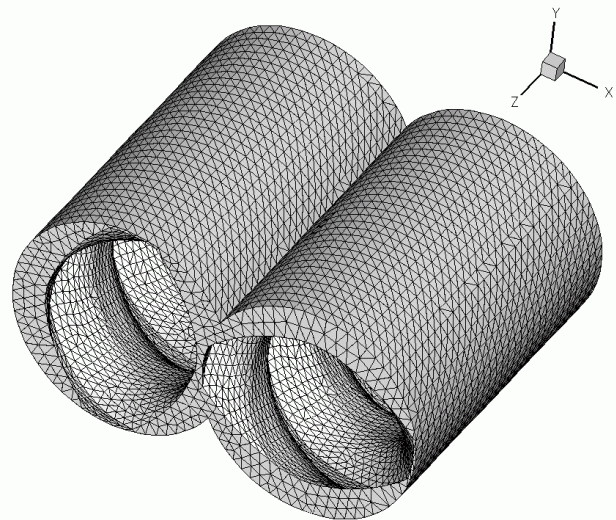
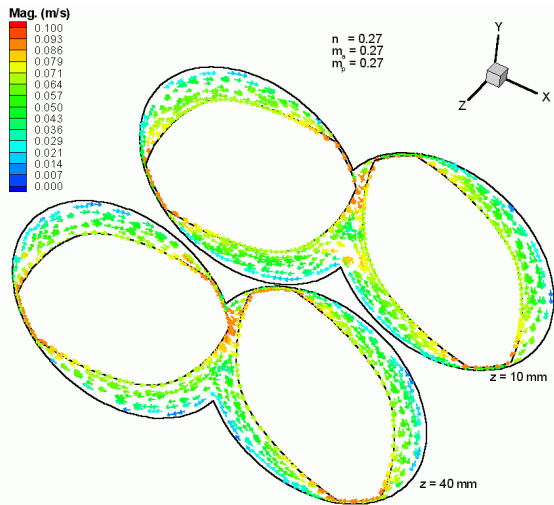
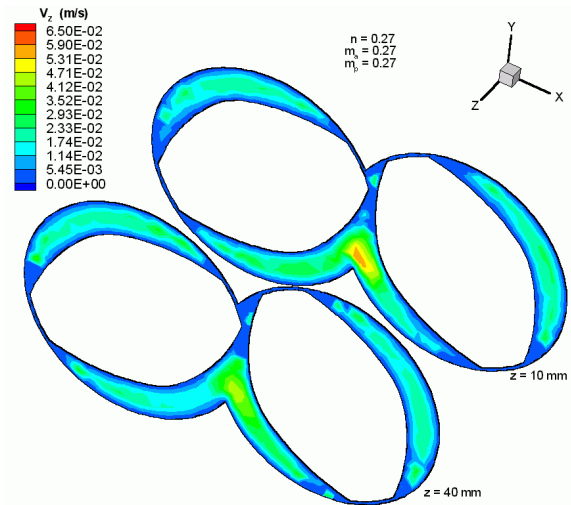


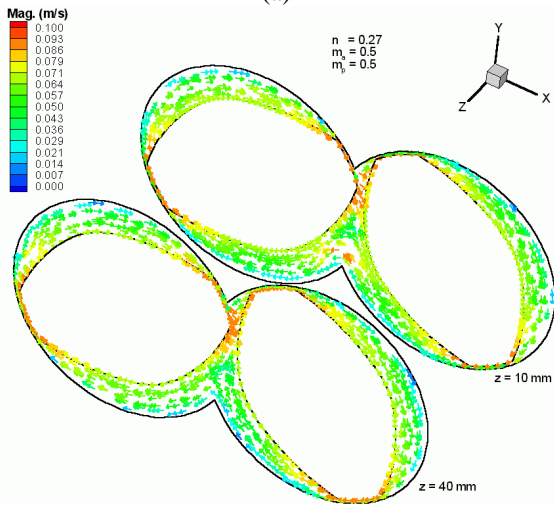
Fig. 2 Finite element mesh used for the flow simulation.



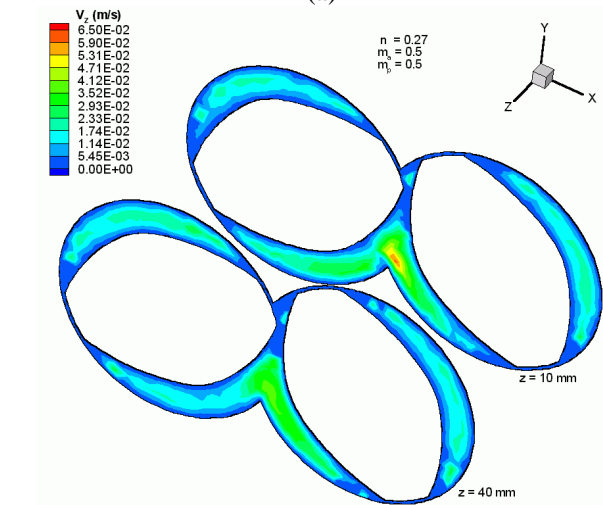
(a)



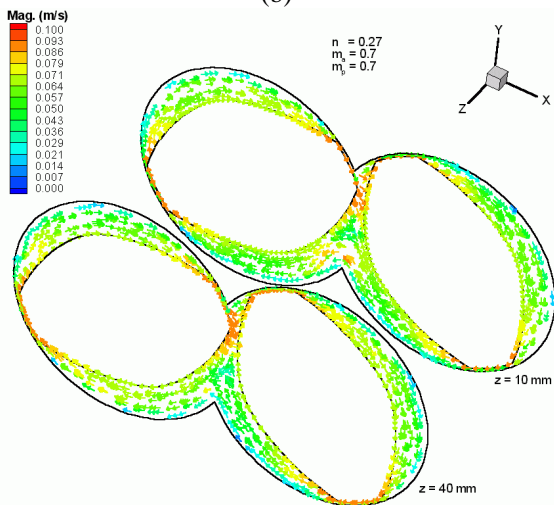
(a)



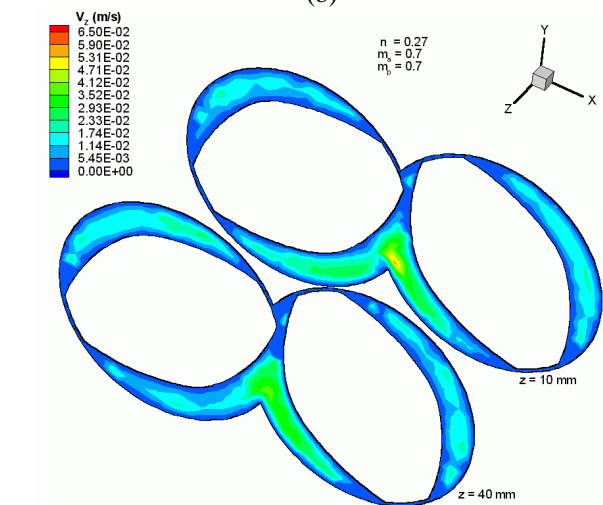
(b)



(b)



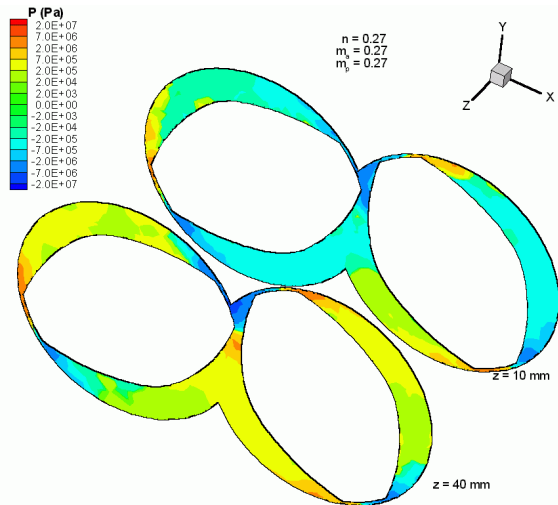
(c)



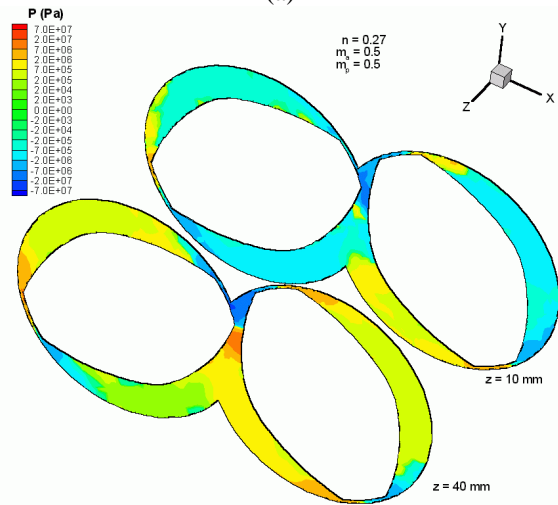
(c)

Fig. 3 Velocity distributions in two of the planes perpendicular to the axis of the twin-screw extruder. Elongational power-law index is (a) 0.27, (b) 0.5, (c) 0.7.

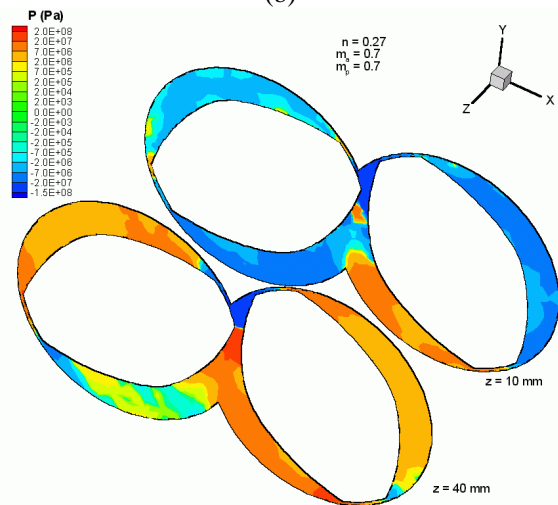
Fig. 4 Axial velocity component in two of the planes perpendicular to the axis of the twin-screw extruder. Elongational power-law index is (a) 0.27, (b) 0.5, (c) 0.7.



(a)

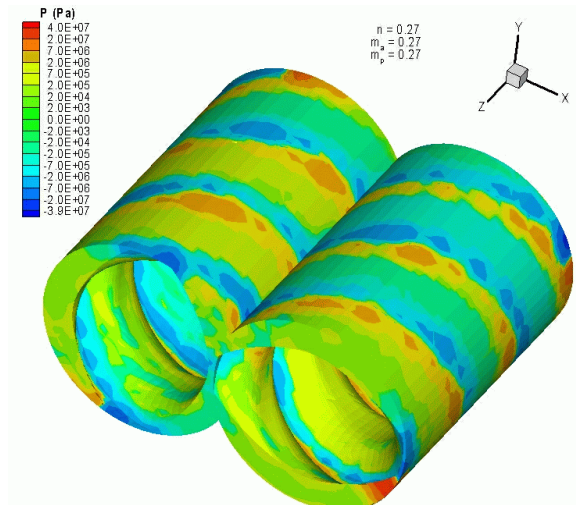


(b)

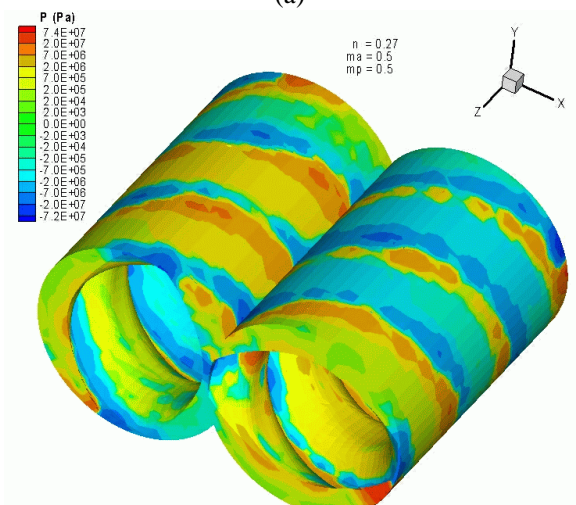


(c)

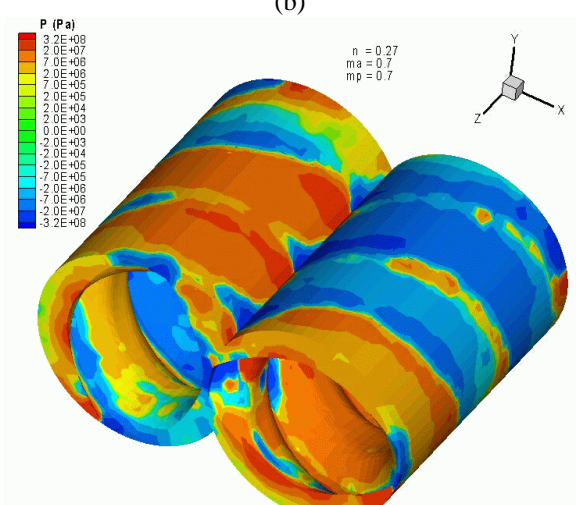
Fig. 5 Pressure distribution in two of the planes perpendicular to the axis of the twin-screw extruder. Elongational power-law index is (a) 0.27, (b) 0.5, (c) 0.7.



(a)



(b)



(c)

Fig. 6 Pressure distribution on the barrel surface and exit of the twin-screw extruder. Elongational power-law index is (a) 0.27, (b) 0.5, (c) 0.7.